Algorithms on time-domain Green function integrated on a cylindrical surface

LI Rui-peng.[1], CHOI Y.M.[2], CHEN Xiao-bo.[1,3], DUAN Wen-yang.[1]

[1]Harbin Engineering University, Harbin, China

[2]Ecole Centrale de Nantes, Nantes, France

[3]Bureau Veritas, Paris, France

Email: liruipeng@hrbeu.edu.cn

Abstract: The Green function method has been widely applied to solve hydrodynamic problems. Both frequency-domain Green function and time-domain Green function, which satisfy not only the governing equation but also the free surface boundary condition, being complex in formulations and numerical evaluations, much efforts have then been made to their computations. Present study focuses on the time-domain Green function which is highly oscillatory and needed in boundary element methods. Integrals involving time-domain Green function and Fourier-Laguerre basis functions integrated on a cylindrical surface are considered. These integrals are derived from a multi-domain method where velocity potentials and corresponding normal derivatives are expanded by Fourier series along circumference and Laguerre functions in vertical direction on a deep cylindrical surface. Time-domain Green function itself is not explicitly computed but its integration needs to be evaluated efficiently and accurately. The multi-fold integrals are analytically integrated and reduced to single ones with respect to wavenumber. To evaluate the wavenumber integrals, contour integrals are introduced in detail and numerical results are given in this paper.

Key words: Time-domain Green function; Fourier-Laguerre expansions; Highly oscillatory integrals; Contour integrals.

1 Introduction

We are concerned here with the evaluation of oscillatory infinite integrals of the form:

$$\int_0^\infty f(k)J_m(ak)J_n(bk)\sin(t\sqrt{k})\mathrm{d}k\,, \tag{1}$$

where (m, n) are nonnegative integer constants, (a, b, t) are positive real constants and $J_n(\cdot)$ is the n-th order Bessel function of the first kind. Integrals such as (1) occur in the time-domain multi-domain method developed in Chen et al. (2018)[1], in which a cylindrical control surface is introduced to divide the whole fluid domain into inner domain and outer domain. On the cylindrical surface, the velocity potential and its normal derivative are expanded by Fourier-Laguerre series. It is of significance to note that the free-surface Green function is not explicitly evaluated but its integration over the control surface needs to be computed instead. Integrals given by (1) are associated with the memory term of transient free-surface Green function and the case of a=b=1 can be obtained from the integral boundary equation in the sense of Galerkin collocation.

Lucas (1995)[2] have considered the simpler problem of evaluating integrals of the form:

$$\int_0^{\infty} f(k) J_m(ak) J_n(bk) dk \,. \tag{2}$$

Though it is claimed that the method can be applied to infinite integrals involving products of more than two Bessel functions of general order and/or sine or cosine function, no example is given. The method will be extended to cope with (1) in this paper and a rather different method will also be presented in the complex plane.

2 Evaluations of oscillatory integrals along the real axis

Decompose the whole integral in (1) into two parts:

$$I_{mn}(a,b,t) = \int_0^{y\max} f(k)\Lambda(k)\mathrm{d}k + \int_{y\max}^{\infty} f(k)\Lambda(k)\mathrm{d}k \,, \tag{3}$$

where the choice of $y\max$ will be discussed later and $\Lambda(k)$ is defined by:

$$\Lambda(k) = J_m(ak) J_n(bk)\sin(t\sqrt{k}) \,. \tag{4}$$

The oscillatory $\Lambda(k)$ can be further split and given by:

$$\Lambda(k) = \sum_{j=1}^{4} B_{mn}^{(j)}\left(k;a,b,t\right), \tag{5}$$

with $B_{mn}^{(j)}(k;a,b,t)$ defined by:

$$\begin{pmatrix} B_{mn}^{(1)}\left(k;a,b,t\right) \\ B_{mn}^{(2)}\left(k;a,b,t\right) \end{pmatrix} = \frac{1}{2}\left[J_{mn}^{+}\left(k;a,b\right)\sin\left(t\sqrt{k}\right) \mp Y_{mn}^{-}\left(k;a,b\right)\cos\left(t\sqrt{k}\right)\right], \tag{6a}$$

$$\begin{pmatrix} B_{mn}^{(3)}\left(k;a,b,t\right) \\ B_{mn}^{(4)}\left(k;a,b,t\right) \end{pmatrix} = \frac{1}{2}\left[J_{mn}^{-}\left(k;a,b\right)\sin\left(t\sqrt{k}\right) \mp Y_{mn}^{+}\left(k;a,b\right)\cos\left(t\sqrt{k}\right)\right], \tag{6b}$$

where $B_{mn}^{(j)}(k;a,b,t)$ and $B_{mn}^{(j)}(k;a,b,t)$ are defined by:

$$J_{mn}^{\pm}\left(k;a,b\right) = \frac{1}{2}\left[J_m\left(ak\right)J_n\left(bk\right) \pm Y_m\left(ak\right)Y_n\left(bk\right)\right], \tag{7a}$$

$$Y_{mn}^{\pm}\left(k;a,b\right) = \frac{1}{2}\left[J_m\left(ak\right)Y_n\left(bk\right) \pm Y_m\left(ak\right)J_n\left(bk\right)\right], \tag{7b}$$

where $Y_n(\cdot)$ is the n-th order Bessel function of the second kind. To avoid large magnitudes of $Y_m(ak)Y_n(bk)$ due to the singularity at k=0 for $Y_m(ak)$ and $Y_n(bk)$, $y$max in (3) is selected such that there is only a finite number of oscillations in [0, *y*max] where an adaptive method is easy to be applied. As suggested in Lucas (1995)[2], the largest of the first zeros of $Y_m(ak)$ and $Y_n(bk)$ can be chosen to be the *y*max.

Substituting (4) into the second integral on the right-hand side of (3), we have:

$$\int_{y\max}^{\infty} f(k)\Lambda(k)\mathrm{d}k=\sum_{j=1}^{4} S_{mn}^{(j)}(a,b,t), \tag{8}$$

with $S_{mn}^{(j)}(a,b,t)$ defined by:

$$S_{mn}^{(j)}(a,b,t)=\int_{y\max}^{\infty} f(k)B_{mn}^{(j)}(k;a,b,t)\,\mathrm{d}k\,. \tag{9}$$

Using asymptotic expressions for large k,

$$\begin{pmatrix} J_n(ak) \\ Y_n(ak) \end{pmatrix} \sim \sqrt{\frac{2}{\pi ak}} \begin{pmatrix} \cos \\ \sin \end{pmatrix}\left(ak-\frac{n\pi}{2}-\frac{\pi}{4}\right), \tag{10}$$

it can be shown that, provided $k \gg 1$,

$$\begin{pmatrix} B_{mn}^{(1)}(k;a,b,t) \\ B_{mn}^{(2)}(k;a,b,t) \end{pmatrix} \sim \frac{A_0}{2}\begin{pmatrix} \sin \\ -\sin \end{pmatrix}\left[(a-b)k\pm t\sqrt{k}-\frac{\pi}{2}(m-n)\right], \tag{11a}$$

$$\begin{pmatrix} B_{mn}^{(3)}(k;a,b,t) \\ B_{mn}^{(4)}(k;a,b,t) \end{pmatrix} \sim \frac{A_0}{2}\begin{pmatrix} -\sin \\ \sin \end{pmatrix}\left[(a+b)k\mp t\sqrt{k}-\frac{\pi}{2}(m+n+1)\right], \tag{11b}$$

with $A_0=1\big/(k\pi\sqrt{ab})$. The phase function in (11) can be written with the form of:

$$\Theta(k)=\sigma k\pm t\sqrt{k}-\chi\,. \tag{12}$$

Stationary points can be observed in Figure 1, locating at

$$k_0=\left(\frac{t}{2\sigma}\right)^2, \tag{13}$$

which are positive roots of $\Theta^{'}(k)=0$. The zeros of $B_{mn}^{(j)}(k;a,b,t)$ are denoted by k_i. $S_{mn}^{(j)}(a,b,t)$ has been studied by Choi (unpublished), who showed the decompositions:

$$S_{mn}^{(2,3)}(a,b,t)=\int_{y\max}^{k_0} f(k)B_{mn}^{(2,3)}(k;a,b,t)\,dk+S^{(2,3)}+R_{23,\infty}^{(2,3)}, \tag{14a}$$

$$S_{mn}^{(1,4)}(a,b,t)=\int_{y\max}^{k_0} f(k)B_{mn}^{(1,4)}(k;a,b,t)\,dk+R_{14,\infty}^{(1,4)}, \tag{14b}$$

where it is assumed *a*>*b*, indicating stationary points will be appeared in $S_{mn}^{(2,3)}(a,b,t)$, and

$$S^{(2,3)}=\sum_{\ell=0}^{l} b_{2\ell}^{(2,3)},\ \ b_{\ell}^{(j)}=\int_{k_\ell}^{k_{\ell+2}} f(k)B_{mn}^{(j)}(k;a,b,t)\,\mathrm{d}k\,, \tag{15a}$$

$$R_{23,\infty}^{(j)}=\lim_{K\to\infty}\sum_{\ell=0}^{K} b_{2(l+1)+2\ell}^{(j)} \quad \text{and} \quad R_{14,\infty}^{(j)}=\lim_{K\to\infty}\sum_{\ell=0}^{K} b_{2\ell}^{(j)}\,. \tag{15b}$$

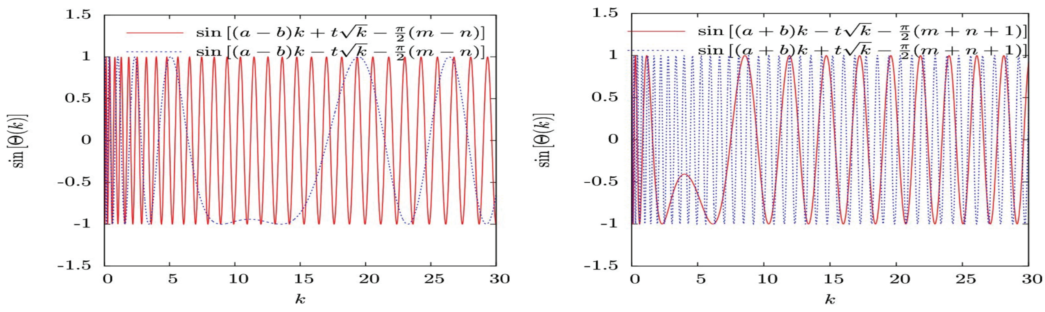

Figure 1 Oscillatory behavior of $\sin[\Theta(k)]$ with m=n=0, a=4, b=1 and t=20.

The infinite series summation may be accelerated by extrapolation, such as ε-algorithm and modified W-transformation used in Lucas (1995)[2]. The modified W-transformation to evaluate $g(k)$ over [a, ∞] are:

$$F(k_s)=\int_a^{k_s} g(k)\mathrm{d}k\,,\ \ \Psi(k_s)=\int_{k_s}^{k_{s+1}} g(k)dk\,,\ \ M_{-1}^{(s)}=F(k_s)/\Psi(k_s)\,,\ \ N_{-1}^{(s)}=1/\Psi(k_s)\,,$$

$$M_p^{(s)}=(M_{p-1}^{(s)}-M_{p-1}^{(s+1)})/(k_s^{-1}-k_{s+p+1}^{-1})\,,\ \ N_p^{(s)}=(N_{p-1}^{(s)}-N_{p-1}^{(s+1)})/(k_s^{-1}-k_{s+p+1}^{-1})\,,$$

$$W_p^{(s)}=M_p^{(s)}/N_p^{(s)}\,,$$

for s={0,1,…} and p={0,1,…} and k_s are zeros of $g(k)$ after a. The final $W_p^{(s)}$ will give the integral results. More details on this can be referred to Sidi (1988)[3].

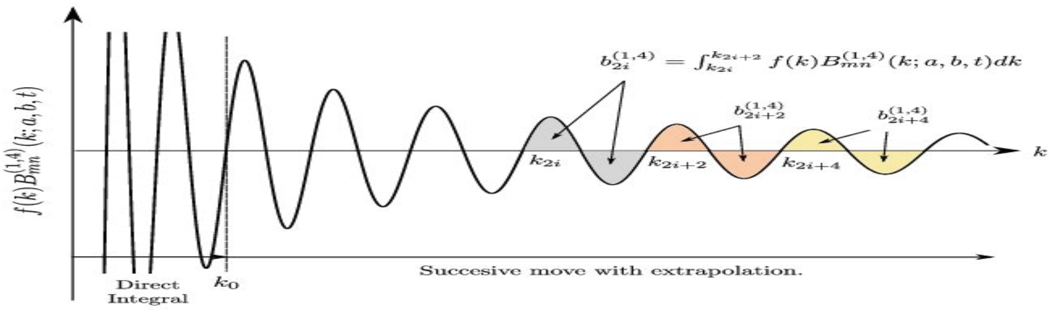

(a) Integrand containing no stationary point.

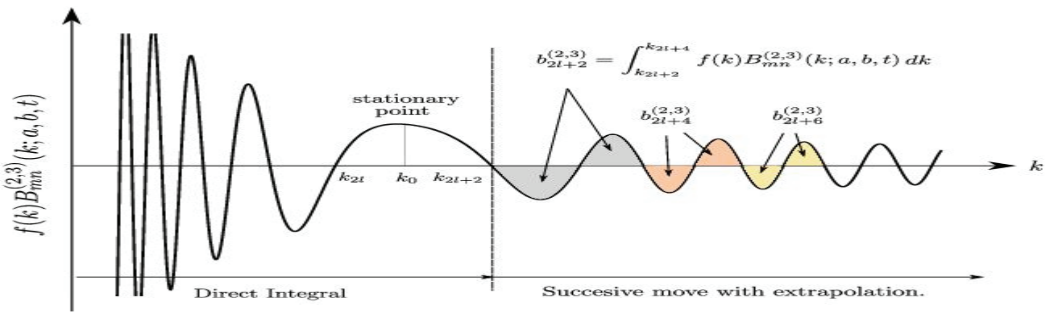

(b) Integrand containing a stationary point.

Figure 2 Evaluation procedure with the extrapolation method for integrals without and with a stationary point.

The determination of zeros k_i in (15) is of significance to the extrapolation acceleration. However, as illustrated in Figure 2, the stationary points shown in (13) make the present integral much more complicated than those only containing products of dual Bessel functions in (2) where there is no stationary point. By using asymptotic expressions given in (11), zeros can be approximately found by increasing phases by π, while a special attention is needed in the vicinity of the phase related with stationary points.

3 Evaluations of oscillatory integrals in complex plane

A rather different numerical method proposed in Chen and Li (2019)[4] can be extended to the evaluations of (1). To consider specified integrals appeared in Chen et al. (2018)[1], define $\beta=\sqrt{k}$ and let a=1, h=b≥1 , $y$max= k_i (here k_i is different from the definition k_i in previous section). The second integral on the right-hand side of (3) is then expressed by:

$$I_\infty\left(h,t\right)=\int_{k_1}^{\infty} f(k)J_m(k)J_n(kh)\sin(\beta t)\mathrm{d}k\,. \tag{16}$$

By substituting the followings into (16),

$$J_m(k)=\frac{1}{2}\left[H_m^{(1)}(k)+H_m^{(2)}(k)\right] \text{ and } \sin(\beta t)=\frac{e^{i\beta t}-e^{-i\beta t}}{2i}, \tag{17}$$

where $H_m^{(1)}(\cdot)$ and $H_m^{(2)}(\cdot)$ are m-th order Hankel function of the first and second kind, respectively. The infinite integral (16) can be rewritten as:

$$I_\infty(h,t)=\Re\left[\frac{1}{4i}\left(I_\infty^A-I_\infty^B+I_\infty^C-I_\infty^D\right)\right], \tag{18}$$

in which,

$$I_\infty^A=\int_{k_1}^{\infty} f^A(k)e^{ikx^+ +i\beta t}\mathrm{d}k \text{ and } I_\infty^B=\int_{k_1}^{\infty} f^B(k)e^{ikx^+ -i\beta t}\mathrm{d}k\,, \tag{19a}$$

$$I_\infty^C=\int_{k_1}^{\infty} f^C(k)e^{ikx^- +i\beta t}\mathrm{d}k \text{ and } I_\infty^D=\int_{k_1}^{\infty} f^D(k)e^{ikx^- -i\beta t}\mathrm{d}k\,, \tag{19b}$$

where $x^{\pm}$=h±1 and the amplitude functions are defined by:

$$f^A(k)=f^B(k)=f(k)\overline{H}_m^{(1)}(k)\overline{H}_n^{(1)}(kh),\ \ f^C(k)=f^D(k)=f(k)\overline{H}_m^{(2)}(k)\overline{H}_n^{(1)}(kh), \tag{20}$$

where $\overline{H}_m^{(j)}(\cdot)$ is defined as:

$$\overline{H}_m^{(j)}(z)=H_m^{(j)}(z)e^{-i(3-2j)z} \text{ with } j=1,2. \tag{21}$$

The integrals in (19) can be summarized to the following two kinds:

$$I^{\pm}(x,t)=\int_{k_1}^{\infty} f(k)e^{i(kx\pm\beta t)}\mathrm{d}k\,. \tag{22}$$

Following the work in Chen and Li[4], the phase function in (22) can be further arranged by:

$$kx\pm\beta t=\left[k\left(\frac{2x}{t}\right)^2\pm2\sqrt{k}\left(\frac{2x}{t}\right)+1\right]\left(\frac{t^2}{4x}\right)-\left(\frac{t^2}{4x}\right), \tag{23}$$

with x>0 and t>0. The change of integral variable

$$u=\sqrt{k}\left(2x/t\right) \quad \text{inversely} \quad k=u^2t^2/(4x^2)=u^2\tau/x, \tag{24}$$

is of interest, and define $\tau=t^2/(4x)$. Therefore, $I^{\pm}(x,t)$ in (22) may be rewritten as:

$$I^+(x,t)=e^{-i\tau}(2\tau/x)\int_{u_1}^{\infty}g(u)e^{i\tau(1+u)^2}\mathrm{d}u,\ I^-(x,t)=e^{-i\tau}(2\tau/x)\int_{u_1}^{\infty}g(u)e^{i\tau(1-u)^2}\mathrm{d}u, \tag{25}$$

with $u_1=\sqrt{k_1}(2x/t)$ and g(u) is defined by $g(u)=uf(u^2\tau/x)$.

Consider the integral associated with $e^{i\tau(1+u)^2}$,

$$I_1=\int_{u_1}^{\infty}g(u)e^{i\tau(1+u)^2}\mathrm{d}u, \tag{26}$$

and perform a change of integral variable $w=(1+u)^2$ inversely $u=\sqrt{w}-1$. For $w\geq w_1^+$ with $w_1^+=(1+u_1)^2$. The integral in (26) can then be transformed to:

$$I_1=\int_{w_1^+}^{\infty}g(\sqrt{w}-1)\frac{e^{i\tau w}}{2\sqrt{w}}dw. \tag{27}$$

As shown in Figure 3, integrals along complete contour are defined by that I_1 along the real w-axis, that $I_{1\infty}$ along the one quarter-circle path of radius $w_m\rightarrow\infty$ and that I_{i1} along the vertical path with $\Re\{w\}=w_1^+$. The sum of them is zero according to the theorem of Cauchy on the complex contour integral. Since $I_{1\infty}=0$ along the one-quarter-circle path of radius $w_m\rightarrow\infty$ according to Jordan's Lemma, we have:

$$I_1=-I_{i1}=\frac{i}{2}e^{i\tau w_1^+}\int_0^{\infty}\frac{g(\sqrt{w_1^++ip}-1)}{\sqrt{w_1^++ip}}e^{-\tau p}\mathrm{d}p. \tag{28}$$

Furthermore,

$$I^+=e^{-i\tau}(2\tau/x)I_1=\frac{i}{x}e^{i\tau(w_1^+-1)}\int_0^{\infty}\frac{g(\sqrt{w_1^++ip/\tau}-1)}{\sqrt{w_1^++ip/\tau}}e^{-p}\mathrm{d}p, \tag{29}$$

which is well suited for numerical computation since the integrand is exponentially decreasing with increasing p for any finite $\tau>0$.

The second integral is associated with $e^{i\tau(1-u)^2}$ for $u_1\geq1$,

$$I_2=\int_{u_1}^{\infty}g(u)e^{i\tau(1-u)^2}\mathrm{d}u. \tag{30}$$

Similarly, we make the change of integral variable, $w=(1-u)^2$ inversely $u=1+\sqrt{w}$ for $w\geq w_1^-$ with $w_1^-=(1-u_1)^2$. The integral in (30) can be rewritten as:

$$I_2=\int_{w_1^-}^{\infty}g(1+\sqrt{w})\frac{e^{i\tau w}}{2\sqrt{w}}\mathrm{d}w. \tag{31}$$

The contour is depicted in Figure 4 and we have:

$$I_2 = \frac{i}{2} e^{i\tau w_1^-} \int_0^{\infty} \frac{g(\sqrt{w_1^- + ip} + 1)}{\sqrt{w_1^- + ip}} e^{-\tau p} dp \,. \tag{32}$$

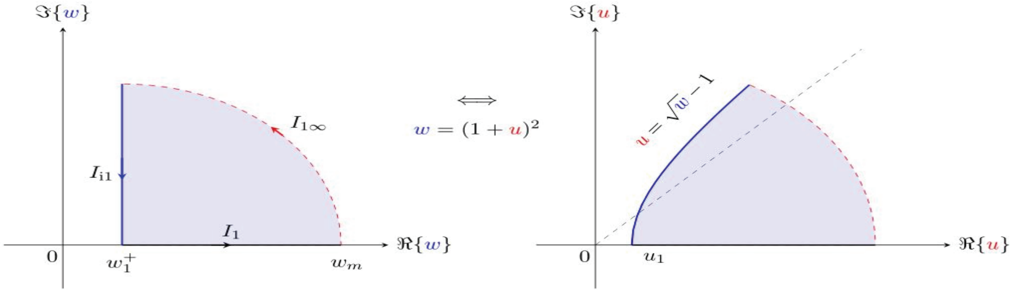

Figure 3 Contour I_1 in the complex w-plane (left) and its mapping in the complex u-plane (right) by $u = \sqrt{w} - 1$ for w from w_1^+ to ∞ with $w_1^+ = (1+u_1)^2$.

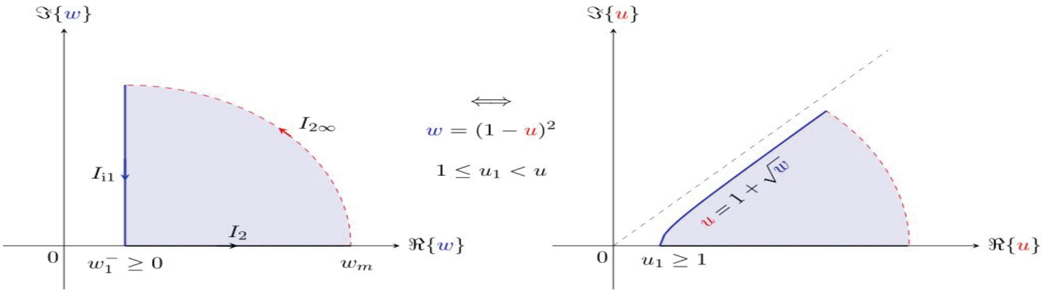

Figure 4 Contour I_2 in the complex w-plane (left) and its mapping in the complex u-plane (right) by $u = \sqrt{w} + 1$ for w from w_1^- to ∞ with $w_1^- = (1-u_1)^2$ and $u_1 \geq 1$.

There is a complementary integral for $u_1 < 1$,

$$I_3 = \int_{u_1}^{1} g(u) e^{i\tau(1-u)^2} \mathrm{d}u \,. \tag{33}$$

Start with a change of the integral variable $w=(1-u)^2$ inversely $u = 1 - \sqrt{w}$. The integral in (33) can be rewritten as:

$$I_3 = \int_{w_1^-}^{0} g(1-\sqrt{w}) \frac{e^{i\tau w}}{-2\sqrt{w}} \mathrm{d}w \,, \tag{34}$$

with $w_1^- = (1-u_1)^2$. The contour is depicted in Figure 5 and we have:

$$I_{i0} = -\frac{i}{2} \int_0^{\infty} \frac{g(1-\sqrt{ip})}{\sqrt{ip}} e^{-\tau p} \mathrm{d}p = -\frac{\sqrt{\tau}}{\tau} e^{i\pi/4} \int_0^{\infty} g(1-\sqrt{i/\tau}\, p) e^{-p^2} \mathrm{d}p \,, \tag{35a}$$

$$I_{i1} = \frac{i}{2} e^{i\tau w_1^-} \int_0^\infty \frac{g(1-\sqrt{w_1^- + ip})}{\sqrt{w_1^- + ip}} e^{-\tau p} \mathrm{d}p \,. \tag{35b}$$

Furthermore,

$$I_3 = \sqrt{i/\tau} \int_0^\infty g(1-\sqrt{i/\tau}\, p) e^{-p^2} \mathrm{d}p - \frac{i}{2\tau} e^{i\tau w_1^-} \int_0^\infty \frac{g(1-\sqrt{w_1^- + ip/\tau})}{\sqrt{w_1^- + ip/\tau}} e^{-p} \mathrm{d}p \,. \tag{36}$$

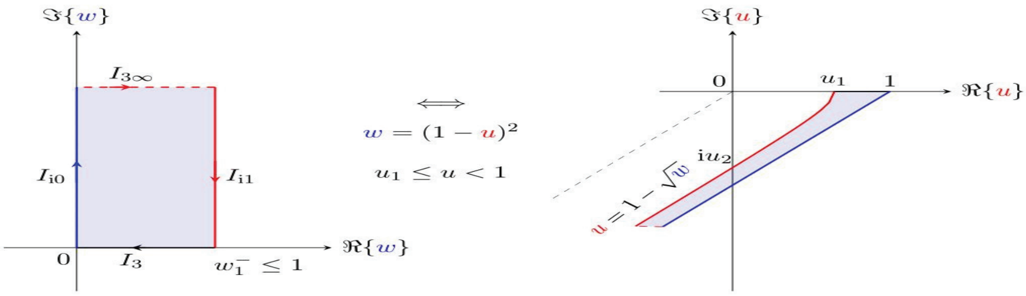

Figure 5 Contour I_3 in the complex w-plane (left) and its mapping in the complex u-plane (right) by $u = 1-\sqrt{w}$ for w from w_1^- to 0 with $w_1^1 = (1-u_1)^2$ for $u_1 < 1$. The point iu_2 with $u_2 = -\sqrt{u_1(2-u_1)}$ is the intersection of the path with axis $\Im\{u\}$.

4 Numerical results and concluding remarks

Though algorithms on transient Green function have been studied in many literatures, the time-domain Green function together with basis functions integrated on analytical surface has not been studied. The integrated time domain Green function can be simplified to a class of highly oscillatory integrals involving the products of dual Bessel functions and a sine function. We have considered these integerals by extending the methods proposed in Lucas (1995)[2] and Chen and Li (2019)[4], respectively. Numerical results are illustrated in Figure 6, provided that $f(k) = \sqrt{k}(k+1/2)^{-1}$. The left is for (*a*=1, *t*=20) and b varying from 1 to 11. The right is for (*a*=1, *b*=2) and *t* varying from 1 to 51. Values at different orders (*m*=*n*={0,1,2}) are shown by curves.

Compared with the time domain Green function itself and its horizontal derivatives which are shown in Figure 7, the integrated Green function have relatively small amplitudes. This property is hopeful to make the novel time-domain multi-domain method numerically stable, where an analytical control surface is introduced and there is no need to discretize the surface as classical boundary element method.

The evaluation of these highly oscillatory integrals is an essential building block for the complete application of the time-domain multi-domain method. The developed algorithms for evaluating highly oscillatory integrals may be further applied to a large variety of oscillatory integrals appeared in fluid mechanics, electromagnetics and so on.

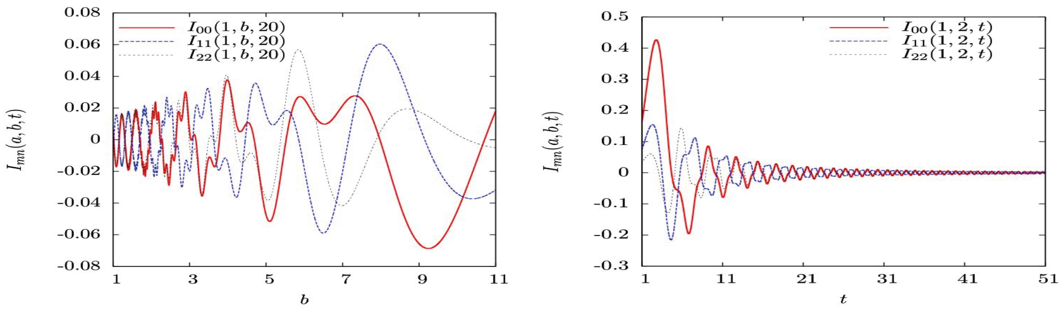

Figure 6 $I_{mn}(a,b,t)$ versus b at t=20 (left) and versus t at b=2 (right). All curves are obtained with a=1 and m=n={0,1,2}.

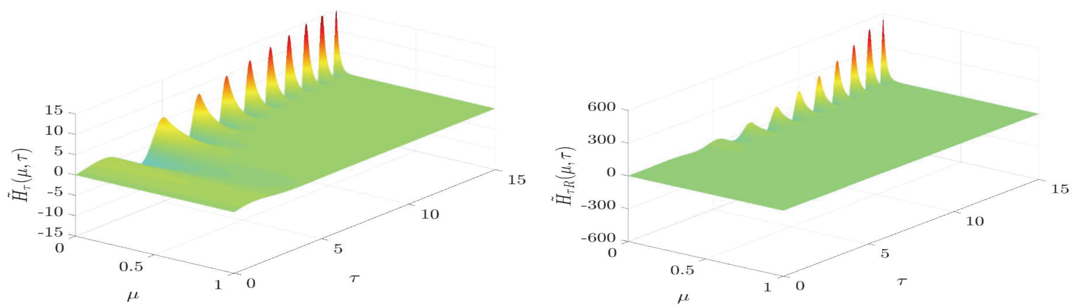

Figure 7 Time domain Green function itself and its horizontal derivatives.

Acknowledgement

This work has been partially supported by the National Natural Science Foundation of China, project number 51779054.

References

1 Chen XB, Liang H, Li RP, Feng XY. Ship seakeeping hydrodynamics by multi-domain method. Proc. 32nd Symposium on Naval Hydrodynamics, 2018.

2 Lucas SK. Evaluating infinite integrals involving products of Bessel functions of arbitrary order. Journal of Computational and Applied Mathematics, 1995, 64: 269–282

3 Sidi A. A user-friendly extrapolation method for oscillatory infinite integrals. Mathematics of Computation, 1988, 51: 249-266

4 Chen XB, Li RP. Reformulation of wavenumber integrals describing transient waves. Journal of Engineering Mathematics, 2019, 115: 121–140